The Yale Undergraduate Research Journal

2020

Investigating factors that affect HIV-1 capsid stability

Max Mao
Yale University

Joshua Temple
Yale University

Recommended Citation

Investigating factors that affect HIV-1 capsid stability

Max Mao[1], Joshua Temple[1]

[1]*Yale University*

Abstract

The HIV capsid, a protein shell composed of monomeric units of CA, forms a fullerene cone that protects HIV's viral genome and enzymes during infection. I am interested in elucidating the factors that influence stability of the capsid shell and capturing the structural interactions between HIV capsid, host restriction factors, and small molecules using biochemical and structural biology techniques. HIV capsid shell was broken down and purified into hexamer and pentamer units for *in vitro* study. Structural assays were performed using X-ray crystallography and biochemical analysis was performed using pelleting assays. By understanding capsid structure with factors that confer stability, treatments can be designed to target the protective HIV capsid before the critical step of viral genome integration with host DNA.

INTRODUCTION

Human immunodeficiency virus 1 (HIV-1) affects millions of people around the world. One particular strain, called HIV-1, infects immune cells such as CD4^{+} T cells and macrophages[1]. If not treated properly, HIV-1 can develop into acquired immunodeficiency syndrome (AIDS) which currently has no cure. Due to its aggressive nature and high-replication rate, HIV-1 is able to circumvent innate host cellular defense mechanisms. In a mature HIV-1 virion, the viral genome and its vital accessory proteins and enzymes are housed within a conical lattice structure known as the capsid. The capsid is composed of a protein shell of monomers called CA protein which polymerize to form ~200 hexamers and 12 pentamers per fullerene cone. The capsid facilitates infection by interacting with multiple host cellular factors while simultaneously protecting viral genetic material and thus serves as a therapeutic target before the critical step of genome integration. Each CA

hexamer and pentamer contains an electropositive pore that mediates binding with many small negatively charged molecules. The charged pore, ringed by a one arginine residue per monomer, presents an environment that is known to interact with phosphate moieties of inositol hexaphosphate (IP6[2]) and deoxynucleoside triphosphate (dNTPs[3]) which promotes charge stability and acts as a nucleotide fuel source for the HIV-1 enzyme reverse transcriptase. Small molecule binding to capsid is a relatively recent discovery and is a field where capsid dynamics can be studied. The capsid must maintain a delicate balance by remaining stable enough to protect HIV genetic material while also being able to break apart to allow cDNA to integrate into the host genome. It is important to understand how CA hexamer/CA pentamer structure, and by extension that of the entire capsid lattice, is affected by small molecule binding, which may result in stability changes or larger scale structural alterations.

Using structural biology, which studies the molecular structure and dynamics of biological macromolecules, complex protein interactions and functions can be studied *in vitro*. Former studies using structure-based crystallography, which utilizes fired X-ray beams at a crystalline layer of protein(s) to calculate the structure of a molecule from its diffraction pattern, have not produced high resolution data. Currently, capsid is difficult to visualize on a structural level due to inherent shortfalls in CA hexamer structure determination. When solving the structure of hexamers, electron density from each CA monomer is averaged together due to 6-fold hexameric symmetry in order to increase the signal:noise ratio and gain a higher resolution model. Since the data is symmetrically averaged, anything bound to the hexamer also has its density averaged out six-fold[2], preempting any useful information of asymmetric binding modes of molecules other than CA. IP6, a small molecule, is inherently asymmetric with binding that may induce slight conformational changes in a hexamer that could propagate throughout the lattice of the capsid to trigger larger scale stability and structure changes. Previous work in Dr. Xiong's lab shows that certain binding partners, such as llama nanobodies with cyclophilin A (CypA[4]), can break the six-fold symmetry, potentially allowing for us to visualize any small molecules that may bind asymmetrically. By breaking the six-fold symmetry, we can gain insight into known small molecule binding and potentially discover other small molecules/peptides that may bind similarly or at other sites.

Our lab mimicked the *in vitro* native capsid through disulfide crosslinking technology using established mechanisms[5]. Through the addition of disulfides, we can crosslink individual hexamers together, effectively recapitulating at least the face of the capsid that binding factors see. Previous studies have shown that small molecules, such as fasciculation and elongation protein 1 (FEZ1), containing poly-glutamate binding regions can directly bind to HIV-1 capsid hexamer pores[9]. Molecules such as polyglutamine binding

protein 1 (PQBP1) and poly-E peptide were investigated with hexamer pores due to having similar charged properties as FEZ1. Furthermore, IP6 was used as a binding agent to hexamer and pentamer pores[2]. After purification and capsid assembly, biochemical and structural studies were performed to continue elucidating the molecular details of CA hexamer and CA pentamer. Using studies on the regulation and structural stability of CA hexamer and CA pentamer presents opportunities to develop more rapid and affordable diagnostic tests and drugs against CA, one of the earliest protein biomarkers in HIV infection[8].

EXPERIMENTAL PROCEDURE

Culture and Growth

HIV-1 CA (A14C/E45C; hexamers for tube assembly) or (A14C/E45C/W184A/M185A; soluble hexamers) or (L21C/N22C/W184A/M185A; soluble pentamers) was cloned into pET11a using Nde1/BAMH1 restriction sites and transformed into BL21(DE3) cells. Cells were grown at 37°C and 200 rpm until OD_{600} ~0.6-0.8 and induced with 0.5 mM IPTG at 25°C for 12 hours. Cells were spun in centrifuge at 5000 RPM for 10 minutes and pellets were stored at -80°C.

CA Preparation

Thawed cell pellets were resuspended in 50 mM Tris pH8, 300 mM NaCL, 0.2 mM TCEP and a tablet of cOmplete Mini, EDTA-free protease inhibitor (Roche). Cells were lysed with a microfluidizer at 15000 psi followed by centrifugation for 35 minutes at 15000 RPM. Lysate volume was proportionally combined with ammonium sulfate to achieve 25% total volume saturation at 4°C and stirred in cold room for 2 hours. Lysate mixture was spun 15000 RPM for 20 minutes. Supernatant was decanted and remaining pellet was let to resuspend in 20 mL of S_A buffer (25 mL HEPES pH 6.8, 0.2 mM TCEP) for 4-5 hours. Once pellet was completely

resuspended, resuspension was dialyzed in S_A buffer at 4ºC overnight. The following day, the sample was spun down for 15 minutes at 15000 rpm and purified using HiTrap SP (GE) ion exchange chromatography[5]. Pentamers preps were identical except using a HiTrap Q (GE) column. Purified constructs were finished with gel filtration (S200 PG; GE) to ensure protein was monodisperse. Protein molecular weight and behavior was analyzed using reducing and non-reducing samples on SDS-PAGE.

Soluble CA Assembly

After obtaining uniformly-dispersed CA monomers, CA proteins are transferred into a dialyzer cassette and dialyzed into 50 mM Tris pH 8, 1M NaCl, and 40 mM BME overnight in 4ºC cold room. The following day, cassette was transferred to dialyze in 50 mM Tris, 1M NaCl for two whole days. Finally, cassette dialyzed in 50 mM Tris for a day. Following the four-day assembly process, soluble CA hexamers and pentamers became stably cross-linked and ready for analysis (Figure 1).
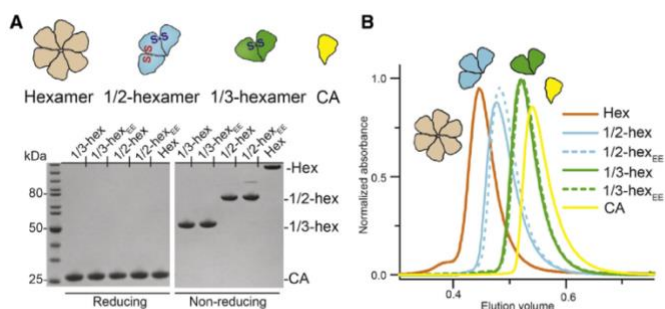

Figure 1.[5] Xiong Lab protocol of *in vitro* engineered capsid hexamer design, assembly, and validation. (A.) HIV-1 capsid hexamers were recreated *in vitro* via disulfide linkages at residues 14 and 45 of CA (A14C/E45C)[5]. Using reducing and non-reducing conditions, hexamers were seen to be composed of monomeric CA protein. Through established capsid protocols, whole hexamers were created and purified using CA. Hexamer complexes were run under reducing and non-reducing gel conditions to reveal dimer, trimer, and hexamer species as designed. (B.) Assembly products were run on size exclusion chromatography and were well-behaved and shown to be monodispersed. Figures obtained from Summer, Brady/Xiong, Yong paper: "Modular HIV-1 Capsid Assemblies Reveal Diverse Host-Capsid Recognition Mechanisms."

Biochemical and structural studies were performed using a variety of CA assemblies[4]: 1) insoluble helical CA tubes, 2) soluble hexamers, created from six CA monomers linked together via disulfide bonds, and 3) soluble pentamers, created from five CA monomers linked together via disulfide bonds. Helical CA tubes, made with cysteine mutations at residues 14 and 45, mimic the inter-hexamer interfaces on the native capsid. After assembly, helical CA tubes labeled CA (14C|45C|WM)were used in pelleting assays to test molecular binding with selective small molecules. Hexamers were created using CA mutant residues at A14C and E45C that were engineered previously in Xiong lab and assembled[5] (Figure 1). The 14C residue of CA forms a disulfide bond with the 45C residue of a neighboring CA to provide stability to hexamers *in vitro*. Utilizing alanine mutations prevents the inter-hexamer polymerization as seen in the 14C|45C|WM mutant. Hexamer mutant constructs were purified and labeled Hexamer 14C|45C|AA (Hex AA). These hexamers were soluble allowing for crystal trays to be set up to characterize their structural interactions with other molecules. Similarly, pentamers were created through cysteine mutations at residues 21 and 22 of CA with residues 21C and 22C of CA forming a disulfide bond to provide stability to pentamers *in vitro*. Pentamer mutant constructs were purified and labeled Pentamer 21C|22C|AA (Pent AA).

Pelleting assay protocol established in Xiong Lab[6] was used to biochemically assess binding interactions between CA tubes and small molecules of interest. The R18 residue of HIV-1 CA A14C/E45C is a target of interest due to that residue being located at the pore, potentially serving as a binding interactor to PQBP1 because of glutamate stretches as shown similarly to FEZ1's binding interaction to the conserved central pore of capsid[9]. Pelleting assay takes advantage of the inherent insolubility of the tubes. Pelleting assay was conducted using CA tubes incubated with PQBP1, a host protein that directly interacts with HIV-1 reverse-transcribed DNA and is a crucial

part of the cGas/IRF3-dependent innate response to HIV[7]. Using maltose-binding protein (MBP) as a negative control, CA tubes and mutant CA tubes were incubated with PQBP1. The mutant CA tubes were at the R18D residue removing the positively charged residue of CA to determine if binding affinity to PQBP1 was affected. Five reactions were created containing the following proteins: 1) MBP, 2) PQBP1, 3) MBP and CA tubes, 4) PQBP1 and CA tubes, 5) PQBP1 and CA R18D tubes. Gel samples were taken from the total incubated sample, the post-centrifugation soluble sample, and from the resuspended insoluble pellet of CA tubes.

Purified Hex AA and Pent AA protein were used for setting up microbatch under oil crystallization screens with various binding partners and small molecules. Hex AA was incubated with CypA, llama nanobody, and IP6. Pent AA crystallization trays were set up in three different forms: 1) Pent AA in Apo-form (Pent AA Apo) at 37.5 uM, 2) Pent AA with CypA at 75 uM, and 3) Pent AA with IP6 at 37.5 uM. Protein solutions were made with proteins of interest and gel filtration buffer (50 mM Tris pH8 and 75 mM NaCl). Crystallization was tested with premade matrix screens including various salt, buffer, and precipitating agents of polyethylene glycol (PEG). The following matrix screens used were NeXtal Classics, Classics Lite, JCSG+, ProComp, and PACT. Crystal trays were initially set up under standard laboratory protocols[4, 5, 6] using a paraffin:silicon oil ratio of 2:1 and a protein:condition solution ratio of 1 µL:1 µL. After obtaining initial crystallization hits, matrix screens were optimized through varying concentrations of protein:condition ratios followed by pH screen optimization and optimization of precipitating agent. Initial crystallization hits were serially seeded into optimized conditions. Protein content verified using light microscopy/birefringent lens, absorption of Coomassie Brilliant Blue dye, ultraviolet fluorescence microscopy, and x-ray crystallography.

RESULTS

Construct Validation

Following established purification and assembly protocols, *in vitro* native capsid hexamers and pentamers were successfully produced. The CA monomer has a molecular weight of 25 kDa and when in its assembled hexamer configuration, the molecular weight expected is 150 kDa. Non-reducing and reducing gel samples of Hex AA indicated that the species was indeed in the right assembled form with a non-reducing band at 150 kDa and reducing at 25 kDa, indicating that all disulfide crosslinks were reduced to form component monomers. Hex AA species also showed high purity via SDS-PAGE (Figure 2). Pent AA constructs were validated through the same process.
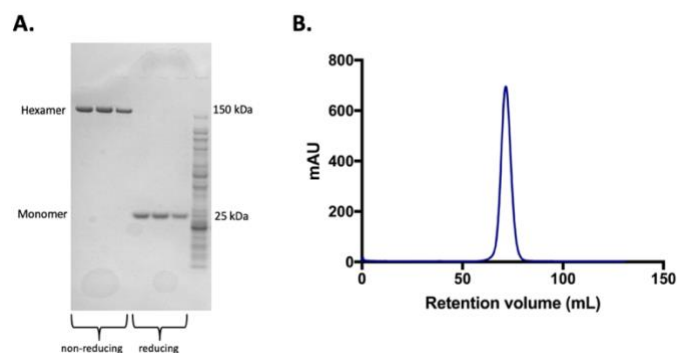

Figure 2. Hexamer AA Purification Validation. (A.) Non-reducing and reducing samples of Hex AA from GF were run on SDS-PAGE to identify the molecular weight of the species. (B.) Post-assembly and purification, Hex AA was run on size-exclusion chromatography/gel filtration column (GF) and showed a uniform, monodispersed peak at the expected retention volume.

Biochemical Assay

Soluble proteins such as MBP and PQBP1 were expected to have higher band density in the soluble gel sample and lesser band density in the pellet gel sample if no significant binding with CA tubes were present. Total, soluble, and pellet fractions were analyzed using SDS-PAGE. Pellet samples show

relatively equal amounts of CA tubes loaded along with equal inputs of MBP and PQBP1 (Figure 3). Negative control of MBP was used as a loading control and was known to have no binding interactions to CA WM/CA R18D. The R18D residue is of interest due to its location in the central pore of capsid. Soluble gel sample appears to show as much PQBP1 protein in supernatant as when PQBP1 was incubated with CA R18D tubes, indicating loss of binding for PQBP1 with the CA R18D tubes. Pellet gel sample shows CA tubes have highest binding affinity to PQBP1, followed by a faint band density for CA R18D tubes. This experiment showed that PQBP1 had a substantial reduction in its binding affinity to CA tubes when the R18D mutation was made (Figure 3).
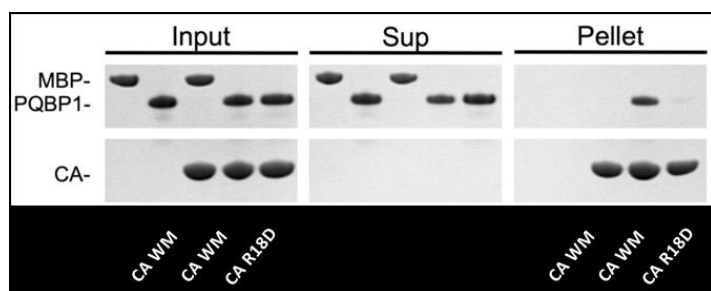

Figure 3. Pelleting assay of CA (WM) tubes/CA R18D tubes with MBP/PQBP1. Total sample (Input) refers to samples taken from the pelleting tubes post-incubation of proteins. Soluble sample (Sup) refers to samples taken of the supernatant from the pelleting tubes post-centrifugation at 14,500 rpm for 15 minutes at 4°C. Pellet sample refers to samples taken from the pelleting tubes after removing supernatant, leaving the insoluble CA tubes with potentially bound proteins. Total, soluble, and pellet fractions were analyzed using SDS-PAGE. Figure created via Microsoft PowerPoint.

Hexamer Crystals

Crystallization hits were obtained from varying matrix screens of ProComp, PACT, and JCSG+. Initial crystal hit of Hex AA with CypA, llama nanobody, and IP6 in ProComp (0.2M Sodium Acetate, 0.1M Sodium Citrate pH 5.5, 10% Polyethylene Glycol 4000) was optimized through varying stoichiometric protein concentration ratios[4] (ranging from 1x to 12x) between CypA and Llama nanobody which improved

crystal lattice structure and created more ordered protein crystals under the same ProComp conditions (Figure 4). Higher resolution crystals from the optimization screen were looped out and sent for x-ray crystallographic data collection. Crystals were cryoprotected with 25% ethylene glycol solutions before frozen in liquid nitrogen. Diffraction data was collected at NE-CAT beamline 24ID-C at the Advanced Photon Source. Diffraction data collected at a resolution of ~7Å was not at a high enough resolution to observe interactions of interest (Figure 4). Crystallization hit from Hex AA with poly-E peptide diffracted at a high-resolution of ~3.5Å (Figure 5).
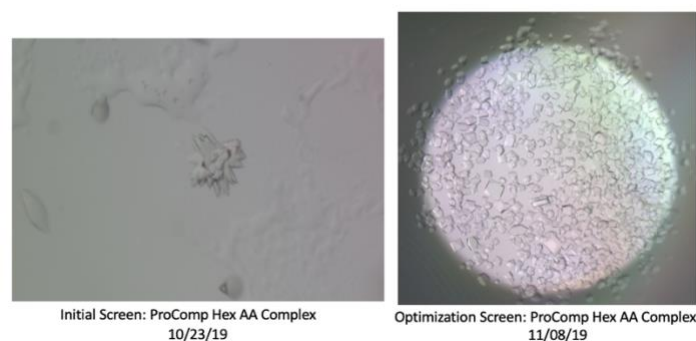

Figure 4. Crystallization using microbatch under oil in ProComp conditions (0.2M Sodium Acetate, 0.1M Sodium Citrate pH 5.5, 10% Polyethylene Glycol 4000) for Hex AA, IP6, llama nanobody, and CypA. Initial screen refers to standard ProComp conditions with a ratio of 1:1 for CypA and nanobody. Optimization screen refers to varying stoichiometric protein ratios between 1x-12x for CypA and nanobody concentrations while keeping ProComp conditions same. Crystals observed under light microscopy and photographed. Pictures formatted on Microsoft PowerPoint.

Figure 5. Crystallization using microbatch under oil for Hex AA

and poly-E peptide. Crystals observed under light microscopy and photographed. Pictures formatted on Microsoft PowerPoint.

Pentamer Crystals

Crystallization hits were obtained from varying matrix screens of JCSG+, PACT, and ProComp. Initial crystal hits in PACT, JCSG+, and ProComp were serially seeded into the same conditions and observed. JCSG+ screens failed to reproduce crystals and were not pursued for further analysis with Pent AA.

Pent AA (APO)

Post-serial seeding, ratio optimizations of protein:condition solution ranging from 0.25x to 3x were performed in matrix screen hits of ProComp (0.1M Magnesium Chloride, 0.1M HEPES pH7, and 15% Polyethylene Glycol 4000; 0.2M Ammonium Sulfate, 0.1M MES pH 6.5, and 20% Polyethylene Glycol 8000) and PACT (0.2M Sodium/Potassium Phosphate and 20% Polyethylene Glycol 3350) (Figure 6). PACT solutions produced jagged, non-uniform and heterogeneous crystals. ProComp condition (0.2M Ammonium Sulfate 0.1M MES pH 6.5, and 20% Polyethylene Glycol 8000) produced the most uniform crystals out of the Pent AA Apo hits. Pent AA Apo hits generally precipitated crystals within 6 days of setting up crystallization trays (Figure 6).
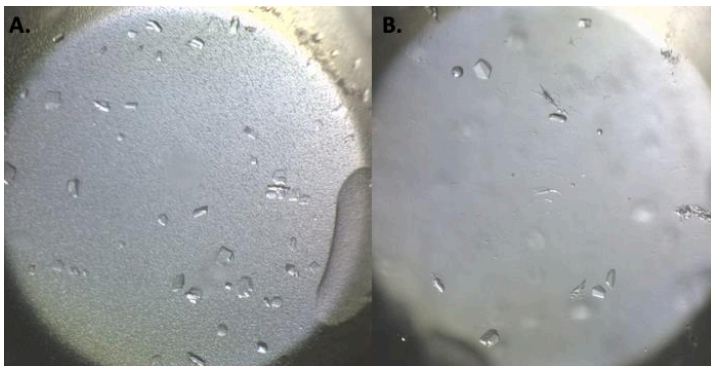

Figure 6. Pent AA (Apo) crystallization using microbatch under oil in ProComp conditions (0.2M Sodium Acetate, 0.1M MES pH 6.5, 20% Polyethylene Glycol 8000). (A.) Left image shows bottom of microbatch under oil drop. (B.) Right image shows surfa view ce of same drop. Crystals observed under light microscopy and photographed. Pictures formatted on Microsoft PowerPoint.

Pent AA with CypA

Initial crystallization hits were in PACT screens (0.2M Sodium Iodide, 0.1M Bis Tris Propane pH 7.5, and 20% Polyethylene Glycol 3350; 0.2M Sodium Iodide, 0.1M Bis Tris propane pH 8.5, and 20% Polyethylene Glycol 3350) and ProComp (0.1M MES pH 6.5 and 15% Polyethylene Glycol 550 MME; 0.1M Magnesium Chloride, 0.1M HEPES pH 7.5, and 10% Polyethylene Glycol 4000). Initial hits were serially seeded into crystal condition hits. Post-serial seeding, ratio optimizations of protein:condition solution ranging from 0.25x to 3x were performed in matrix screen hits of PACT and ProComp. PACT failed to reproduce initial crystallization hits with Pent AA CypA. ProComp condition 0.1M HEPES pH 7.5, and 10% Polyethylene Glycol 4000 produced the most uniform, singular crystals post-ratio optimization. Pent AA with CypA hits generally precipitated crystals within 30 days of setting up crystallization trays.

Pent AA with IP6

Initial crystallization hits were in ProComp screen (0.1M Sodium Citrate pH 5 and 8% Polyethylene Glycol 8000) and PACT screens (0.2M Sodium Chloride, 0.1M MES pH 6, and 20% Polyethylene Glycol 6000; 0.2M Magnesium Chloride, 0.1M HEPES pH 7, and 20% Polyethylene Glycol 6000) (Figure 7). Initial hits were serially seeded into crystal condition hits. Post-serial seeding, ratio optimizations of protein:condition solution ranging from 0.25x to 3x were performed in matrix screen hits of PACT and ProComp. Optimized crystal hits from PACT 0.2M Magnesium Chloride, 0.1M HEPES pH 7, and 20% Polyethylene Glycol 6000 produced the most uniform and singular crystals. Ratio optimization was followed by HEPES pH gradient from 6.0 to pH 8.0 (in increments of 0.2 pH) and percent precipitating agent (10%, 20%, 30% PEG 6000) in combination with standard 0.2M $MgCl_2$. Optimal pH was determined to be 7.4 in combination with 0.2M $MgCl_2$ and 30% PEG 6000. pH optimization was

followed by a 30% PEG screen (ranging PEG 400 to PEG 20000) with protein:condition solution ratios of (1:1, 1:1.5, and 1:2). Pent AA with IP6 hits generally precipitated crystals within 7 days of setting up crystallization trays (Figure 7).
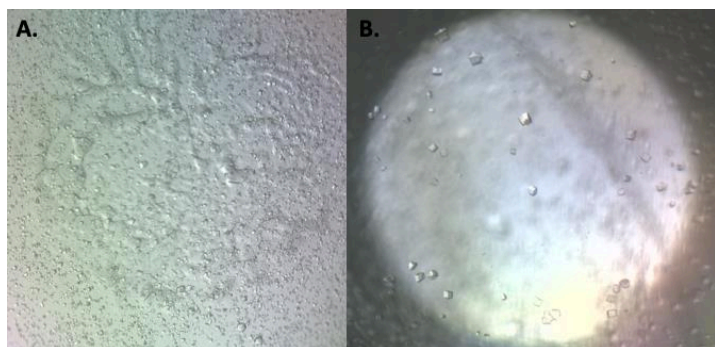

Figure 7. Pent AA with IP6 crystallization using microbatch under oil. (A.) Initial crystal hit for ProComp conditions (0.2M Magnesium Chloride, 0.1M HEPES pH7, and 20% Polyethylene Glycol 6000) observed on 01-22-20. (B.) Crystal hit post-protein:condition ratio/pH/precipitating agent optimization with conditions: 0.2M Magnesium Chloride, 0.1M HEPES pH 7.4, and 30% Polyethylene Glycol 6000 observed on 02-07-20. Crystals observed under light microscopy and photographed. Pictures formatted on Microsoft PowerPoint.

DISCUSSION

Analysis of key binding regions in CA tubes provides novel information on capsid structure and stability. Molecules containing poly-glutamate stretches have been shown to interact with the centrally-charged pore region of capsid such as FEZ1[9]. This indicates a key binding region for small stabilizing molecules. As expected, when the CA tubes were mutated with R18D, there was a loss of binding to PQBP1, a molecule containing similar glutamate stretches (Figure 3). Results indicate that we now know PQBP1 specifically targets the CA hexamer pore. Pelleting assays[6] are currently in progress using mutant residues of PQBP1 to test which regions of PQBP1 interact with CA hexamer pore (Figure 3). Further pelleting assays will be conducted with restriction factors of interest and

small molecules of interest to characterize the capsid lattice structure.

Given that each capsid fullerene cone contains ~200 hexamers, studying the hexamer structure presents opportunities to identify small molecule factors that may stabilize its presence in host organisms. IP6 is an essential HIV pocket factor that prevents capsid collapse with the six negatively charged phosphate groups stabilizing the positively charged arginine ring of hexamers[2]. Hex AA with IP6, CypA, and llama nanobody crystal hits from initial ProComp matrix screen (0.2M Sodium Acetate, 0.1M Sodium Citrate pH 5.5, 10% Polyethylene Glycol 4000) were successfully optimized as shown by the growth in size and density (Figure 4). Due to a variety of external factors, including crystal lattice order, molecular packing and beam intensity from x-ray crystallography, the diffraction data collected at NE-CAT beamline 24ID-C at the Advanced Photon Source was not high resolution. Lack of resolution could be attributed to CypA and llama nanobody creating too dynamic of a lattice to have solid packing and good order for data collection. Poly-E peptide was examined as a potential binding candidate to Hex AA due to having similar glutamate stretches as FEZ1[9] and PQBP1. High-resolution diffraction data of Hex AA with poly-E peptide was obtained at 3.5 Å (Figure 5). Data is currently being processed for structural analysis. Poly-E peptide has a chain of glutamates that was thought to have high binding affinity to the central capsid pore. Our crystallization results indicated that poly-E peptide did indeed bind to the charged hexamer pore. This discovery aligns with prior studies where hexamer pore was shown to bind to poly-glutamate stretches[9]. Further studies include setting repeats of with Hex AA in its most optimized state with variations in pH, temperature, protein concentrations, and molecules present as all of these factors can play a role in the stability and crystal lattice formation. Small molecules of interest including, but not limited to: IP6, various dNTPs, CypA,

llama nanobody, and other phosphate moieties in combination with other matrix screens can be set up.

Each capsid fullerene cone contains 12 pentamers that have points of the highest stress due to being essential for the curvature of the cone. Due to this increased stress, regions in the pentamer could be where capsid initially breaks open to release its viral genome into the host. and thus presents an interesting target to study. Unlike hexamers, pentamers don't have the same symmetry problem since lattices do not allow 5-fold symmetry to propagate. Currently, there are no structures of pentamers with small molecules and presents an interesting target for analysis. First, crystallization trays of the Apo-form of Pent AA were set up in order to understand baseline conditions that affect the stability and structure of them in solution (Figure 6). After setting up various matrix screens, it appeared that Pent AA was generally most stable in pH ranges between 6-7 with higher molecular weight precipitating agents (PEG 6000-8000) at a 20-30% ratio. After months of trial and error with optimization, it is noteworthy that the crystals produced from Pent AA Apo generally remained the same size even after optimization of matrix screens, protein:condition solution, pH, and precipitating agent. The lack of crystal growth and density could be attributed to the lack of molecules present in solution and/or the pentamer structure inhibiting higher ordered lattice packing. CypA with llama nanobody could be used as cofactors to break the six-fold symmetry when bound to Hex AA[4,5]. CypA was a host factor that when combined to llama nanobody and Hex AA allowed for symmetry breaking and the visualization of molecular interactions in capsid hexamers. Pent AA with CypA presented a novel opportunity to characterize a potential interaction between them. After months of optimization from matrix screens, the most ordered crystals produced came from ProComp condition (0.1M $MgCl_2$, 0.1M HEPES pH 7.5, and 10% PEG 4000). Given that IP6 was a stabilizing molecule for Hex AA, Pent AA incubated with IP6 presented an interesting novel target to study (Figure 7). The most ordered Pent AA with IP6 crystals came from PACT condition (0.2M $MgCl_2$, 0.1M HEPES pH 7.4, and 30% PEG 6000). Interestingly, when Pent AA was present with either CypA or IP6, it preferred conditions of magnesium chloride (0.1-0.2M $MgCl_2$) and HEPES (pH 7.4-7.5). The solution conditions between Pent AA CypA and Pent AA IP6 were in fact almost identical. Surprisingly, Pent AA with CypA took the longest time to produce crystals (~30 days) compared to Pent AA Apo or Pent AA IP6 (~6 days). Given that the crystallization trays tested were almost identical aside from the small molecules of interest, I expected the Pent AA crystals to all precipitate at relatively similar time periods. Being that microbatch under oil crystallization techniques allow for the slow evaporation of condition under oil, it is not unreasonable that crystals can be formed at later time periods due to varying evaporation rates that alter protein concentrations present.

Unfortunately, due to the COVID-19 pandemic, novel optimized Pent AA crystals, observed in late February, in Apo-form, with IP6, and CypA could not be shot and analyzed using beam time. Future directions include the continued optimization of Hex AA and Pent AA crystals with higher resolution crystals analyzed using x-ray crystallography. Furthermore, *in vitro* fullerene capsid shells could be created and tested to understand the macromolecular stability of capsid. By obtaining diffraction patterns of capsid crystals, an electron density map and model of the molecular interactions can be created. By continuing to optimize crystals to achieve better resolutions, more precise models of the molecular interactions can be obtained. Ultimately, these models can be used to characterize capsid's metastable condition and further understand how its domains are affected spatial and temporal for novel drug targeting.

ENDNOTES

[1]"About HIV/AIDS | HIV Basics | HIV/AIDS | CDC." *Centers for Disease Control and Prevention*, Centers for Disease Control and Prevention, 14 Aug. 2019.

[2]Mallery, Donna L, et al. "Figures and Data in IP6 Is an HIV Pocket Factor That Prevents Capsid Collapse and Promotes DNA Synthesis." *ELifeSciences.org*, Life Sciences Publications Limited, 31 May 2018.

[3]Jacques, David A, et al. "HIV-1 Uses Dynamic Capsid Pores to Import Nucleotides and Fuel Encapsidated DNA Synthesis." *Nature.com*, Macmillan Publishers Limited, 10 Aug. 2016.

[4]Gerber, Eva E, et al. "CA-targeting nanobody is a tool for studying HIV-1 capsid lattice interactions." *Xiong Laboratory*. 13 July 2019. *Unpublished.*

[5]Summers, Brady, et al. "Modular HIV-1 Capsid Assemblies Reveal Diverse Host-Capsid Recognition Mechanisms." *Cell Host & Microbe*, 203–216. August 14, 2019. Published by Elsevier Ltd.

[6]Smaga, Sarah S, et al. "MxB Restricts HIV-1 by Targeting the Tri-hexamer interface of the Viral Capsid." *Cell Press*, 1234-1245. August 6, 2019. Published by Elsevier Ltd.

[7]Yoh, Sunnie M. *PQBP1 Is a Proximal Sensor of the CGAS-Dependent Innate Response to HIV-1*. Cell/CellPress , 4 June 2015. Published by Elsevier Ltd.

[8]Gray, E. R., et al. "A landscape review of antigen detection for early HIV diagnosis." *AIDS 32,* 2089-2102. 2018.

[9]Huang, Pei-Tzu., et al. "FEZ1 Is Recruited to a Conserved Cofactor Site on Capsid to Promote HIV-1 Trafficking." *Www.cell.com*, Cell Reports, 27 Aug. 2019.